



# Spatial and temporal variabilities of the chlorophyll distribution in the northeastern tropical Pacific: The impact of physical processes on seasonal and interannual time scales

Yoshikazu Sasai <sup>a,\*</sup>, Kelvin J. Richards <sup>b</sup>, Akio Ishida <sup>a</sup>, Hideharu Sasaki <sup>c</sup>

<sup>a</sup> Research Institute for Global Change, Japan Agency for Marine-Earth Science and Technology, 3173-25, Showa-machi, Kanazawa-ku, Yokohama, 236-0001, Japan

<sup>b</sup> International Pacific Research Center, SOEST, University of Hawaii, Honolulu, 96822, USA

<sup>c</sup> Earth Simulator Center, Japan Agency for Marine-Earth Science and Technology, Yokohama, 236-0001, Japan

## ARTICLE INFO

### Article history:

Received 11 August 2011

Received in revised form 19 December 2011

Accepted 30 January 2012

Available online 15 February 2012

### Keywords:

Chlorophyll

Northeastern Tropical Pacific

Physical processes

Seasonal and interannual scale

Eddy-resolving physical–biological model

## ABSTRACT

A global eddy-resolving coupled physical–biological model is used to investigate the seasonal and interannual variabilities of the chlorophyll in the northeastern tropical Pacific during 2000–2007. The seasonal variability of the surface chlorophyll concentration in the model agrees well with satellite ocean color data, except for the equatorial region. High chlorophyll levels off the Gulf of Tehuantepec, Papagayo, and Panama in winter and in the Costa Rica Dome in summer are well reproduced. Production in these areas is controlled by the supply of nitrate rich-waters through vertical mixing and coastal and open ocean upwelling. The variability of the thermocline depth is strongly connected to the seasonal variability of surface chlorophyll. El Niño Southern Ocean (ENSO) variability has a marked effect on the marine ecosystem. The model reproduces the variability of chlorophyll corresponding to the observed ENSO variability. During cold SST anomaly phases (2000, 2001 and 2007), the chlorophyll concentration is considerably higher than other years (2002–2006). Chlorophyll variance is largest off the Gulf of Papagayo and over the Costa Rica Dome where the changes to chlorophyll levels are related to changes in the supply of nitrate rich-waters through vertical mixing and upwelling.

© 2012 Elsevier B.V. All rights reserved.

## 1. Introduction

The eastern tropical Pacific presents a changing physical environment on a range of timescales. Physical features in this region are a strong and shallow thermocline, the Intertropical Convergence Zone (ITCZ) and the wind jets, coastal and equatorial upwelling, the Costa Rica Dome, and eastern boundary and equatorial current systems (e.g., Amador et al., 2006; Fiedler and Talley, 2006; Kessler, 2006; Willett, et al., 2006). These physical features have influence on the temporal and spatial variabilities of the biological environment. The effects of physical processes on biological fields have been investigated using ship and satellite observation data and model results (e.g., Fiedler, 2002a; McClain et al., 2002; Pennington, et al., 2006; Sasai et al., 2007).

The wind jets blow over the Gulfs of Tehuantepec, Papagayo, and Panama, caused by the pressure gradient between the Atlantic and Pacific and accelerated by the narrow passes in the topography of Central America. In fall, winter and early-spring, the strong wind jets develop and cause mixing directly below the axis of the jet, and the wind stress curl in the Ekman upwelling to the southeast of the jet and downwelling to the northwest induced by wind stress curl. As a

consequence the nutrient-rich water is brought to the surface beneath and to the south of the jet, and high levels of chlorophyll develop. Ocean-color satellite images capture three distinct high chlorophyll concentration regions associated with the wind jets (Gonzalez-Silva, et al., 2004; McClain et al., 2002; Müller-Karger and Fuentes-Yaco, 2000). There are distinct filaments and eddies in the Gulf of Tehuantepec and the Gulf of Papagayo generated by the wind jets that extend as far as 900 km offshore. The generated eddies cause the high primary productivity and play an important role in the onshore–offshore exchange of biological material (Müller-Karger and Fuentes-Yaco, 2000). Using a model, Samuels and O'Brien (2008) showed that there is substantial offshore export of organic material in the Gulf of Tehuantepec, particularly during strong wind jets that generates eddies.

Another feature of the eastern tropical Pacific is the Costa Rica Dome, which is a shallow doming of the thermocline. The dome is centered at 9°N, 90°W and expands seasonally to the west in the boreal summer. The characteristics of the feature are influenced by the east–west thermocline ridge associated with the equatorial circulation, surface currents, and its seasonal evolution is affected by the large-scale wind pattern (Fiedler, 2002a; Kessler, 2002). In the Costa Rica Dome, the 20 °C isotherm depth is brought close to the surface: a depth of only 30 m on the annual mean (Fiedler, 2002a). The open-ocean upwelling (about 0.5 m day<sup>-1</sup>) and mixing bring up rich-nutrient waters to the

\* Corresponding author.

E-mail address: [ysasai@jamstec.go.jp](mailto:ysasai@jamstec.go.jp) (Y. Sasai).

euphotic zone and support high biological productivity (Fiedler, 2002a; Sasai et al., 2007).

The interannual variability of the marine ecosystem in the eastern tropical Pacific is dominated by the El Niño Southern Oscillation (ENSO) phenomenon. The physical effects of El Niño involve a deepening of the thermocline and nutricline, with the effect on primary productivity (Pennington et al., 2006) being mainly negative. A La Niña event shallows the depth of the thermocline and nutricline and leads to an increase in primary productivity. The biological effects of ENSO variability in the eastern tropical Pacific have been investigated using hydrographic and satellite data (e.g., Chavez, et al., 1999; Fiedler, 2002b; Pennington et al., 2006; Ryan et al., 2002; Strutton and Chavez, 2000).

The eastern tropical Pacific is in general a nitrogen-limited system (Fiedler et al., 1991). However, the nitrate is not fully utilized by the phytoplankton and nitrate levels remain high in the region. High-nitrate low-chlorophyll (HNLC) conditions occur in the equatorial upwelling and south equatorial current regions, and in the offshore Peru upwelling region (Bruland et al., 2005). A number of hypotheses to explain the HNLC condition have been proposed: trace metal inhibition of phytoplankton growth, grazing, species composition, nitrate and silicate regulation, and iron limitation (e.g., Barber and Ryther, 1969; Chavez, 1989; Dugdale et al., 1995; Landry and Kirchman, 2002; Martin et al., 1994).

In the northeastern tropical Pacific, the gap winds have a large influence on the physical and biological environment. In this study, we investigate the seasonal variability of the marine ecosystem and its relationship to physical processes (e.g., thermocline depth, Costa Rica Dome, Ekman pumping, and mixing) in the northeastern tropical Pacific (with the exception of region close to the equator) using an eddy-resolving physical-biological model forced by the QSCAT wind field. To focus on the nitrogen-limited system in this region, we employ a simple nitrogen-based four-compartment nitrate-phytoplankton-zooplankton-detritus (NPZD) ecosystem model (Oschlies, 2001; Sasai et al., 2006, 2010). We determine the physical controls on the marine ecosystem and examine the spatial response of the marine ecosystem to ENSO variability and which area is a large influence of ENSO.

## 2. Model description

The ocean model is the Ocean general circulation model For the Earth Simulator (OFES) (Masumoto et al., 2004), which is based on the Geophysical Fluid Dynamics Laboratory's Modular Ocean Model (MOM3) (Pacanowski and Griffies, 2000). The model domain ranges from 75°S to 75°N. The horizontal resolution is 0.1°. There are 54 vertical levels, with varying thickness between the levels from 5 m at the surface to 330 m at the maximum depth of 6065 m. Prior to the experiment described here, the physical component of the model was forced by the daily mean NCEP/NCAR reanalysis (Kalnay et al., 1996) for 48 years from 1950 to 1998 after 50 years spin-up under a climatological monthly mean forcing.

The marine ecosystem model is a simple nitrogen-based four-compartment (Nitrate, Phytoplankton, Zooplankton, Detritus) ecosystem model (Oschlies, 2001). The evolution of the biological tracer concentrations in the OFES is governed by an advection-diffusion equation with source and sink terms. The source and sink terms represent the biological activity. The details of the ecosystem model are described in Sasai et al. (2006, 2010). To establish a stable pattern of the biological fields, the biological model is incorporated after a 50-year spin-up with climatology. The biological model coupled with the evolving physical fields was integrated a further 5-year period under the climatological monthly mean forcing. The variability of biological fields has no feedback on the physical fields. The biological fields in the last year of the coupled 5-year integration are used as initial conditions for this simulation.

For the experiment reported here, the coupled physical-biological model is forced by the daily mean surface wind stress data of Quick Scatterometer (QSCAT) and atmospheric daily mean data (heat and salinity fluxes) of the NCEP/NCAR reanalysis from 1999 to 2007. Results are presented for years 2000 to 2007. The simulated phytoplankton concentration ( $\text{mmol N m}^{-3}$ ) is converted to chlorophyll concentration ( $\text{mg m}^{-3}$ ) using a ratio of 1.59 g chlorophyll per mol nitrogen (e.g., Cloern et al., 1995; Fasham et al., 1990; Oschlies, 2001) to compare with the SeaWiFS. To investigate the performance of OFES, we have used the ocean color satellite image data of the Sea-viewing Wide Field-of-View Sensor (SeaWiFS).

## 3. Results

### 3.1. Seasonal cycle

Seasonal variability of the climatological monthly mean surface chlorophyll concentration during 2000–2007 is shown in Fig. 1. Both surface chlorophyll concentrations of SeaWiFS and OFES show patterns that are related to the variability of thermocline depth, coastal upwelling, eddies, and ocean circulation. The annual cycle of the surface chlorophyll concentration is particularly influenced by the thermocline depth variability (Fiedler, 2002a). From January to April, the observations (SeaWiFS) show winter-spring blooms near the coast at the Gulfs of Tehuantepec, Papagayo, and Panama. In winter and early spring, strong wind jets develop over the three Gulfs (Chelton et al., 2000, 2004). These strong wind jets produce vertical mixing and Ekman upwelling (Fig. 2), and nutrient-rich waters are supplied from the subsurface layer to the surface. In May, the observed chlorophyll concentration increases off the Gulf of Papagayo with the shoaling thermocline depth. From July to September, the observed surface chlorophyll increases offshore along the shoaling thermocline ridge, with a local maximum corresponding very closely to the Costa Rica Dome (Fiedler, 2002a). Coastal blooming begins again in October in the Gulf of Tehuantepec and December in the Gulfs of Papagayo and Panama, when the winds jets initiate mixing of surface waters near the coast.

The simulated surface chlorophyll captures the dominant annual cycle of the observed surface chlorophyll, especially, the winter-spring bloom at the three Gulfs, and open-ocean blooming in summer off the Gulf of Papagayo (Fig. 1). In the model, during January–April, the vertical mixing and Ekman upwelling (Fig. 2) by the strong wind jets over the three Gulfs lift up the nitrate-rich waters to the surface layer and the winter-spring bloom occurs (Samuelson and O'Brien, 2008; Sasai et al., 2007). During May–September, the shallow thermocline dome formed by the wind forcing (the Costa Rica Dome) maintains the open-ocean blooming off the Gulf of Papagayo. During October–December, the model shows a high chlorophyll concentration along 8°N (the Costa Rica Dome). However, the SeaWiFS data shows that the fall bloom ceases in November.

The seasonal variability of the simulated surface chlorophyll concentration (Fig. 1) mainly reflects the change in the thermocline depth (20 °C isotherm depth) (Fig. 3). In winter, the strong gap wind jets over the three Gulfs cause Ekman upwelling to the south of jets (Fig. 2). There is strong upwelling ( $> 10 \times 10^{-6} \text{ m s}^{-1}$ , or  $25 \text{ m month}^{-1}$ ) in each of the three Gulfs. In summer, the ITCZ shifts to around 8°N and the associated strong Ekman upwelling ( $5 \times 10^{-6} \text{ m s}^{-1}$ , or  $12 \text{ m month}^{-1}$ ) is dominant in the open-ocean signal. The Ekman pumping contributes to the shoaling of thermocline in winter, but the influence is weak in other seasons. The annual cycle of the thermocline depth has a local minimum near 9°N 90°W (the Costa Rica Dome) (Fig. 3). Using hydrographic data, the annual cycle or seasonal evolution the Costa Rica Dome was examined by Fiedler (2002a) (see also Fig. 7 of Kessler, 2006). The model reproduces the observed seasonal variability of the hydrographic data (Fiedler, 2002a), especially, the shoaling and deepening of the thermocline with the evolution of the Costa Rica Dome.

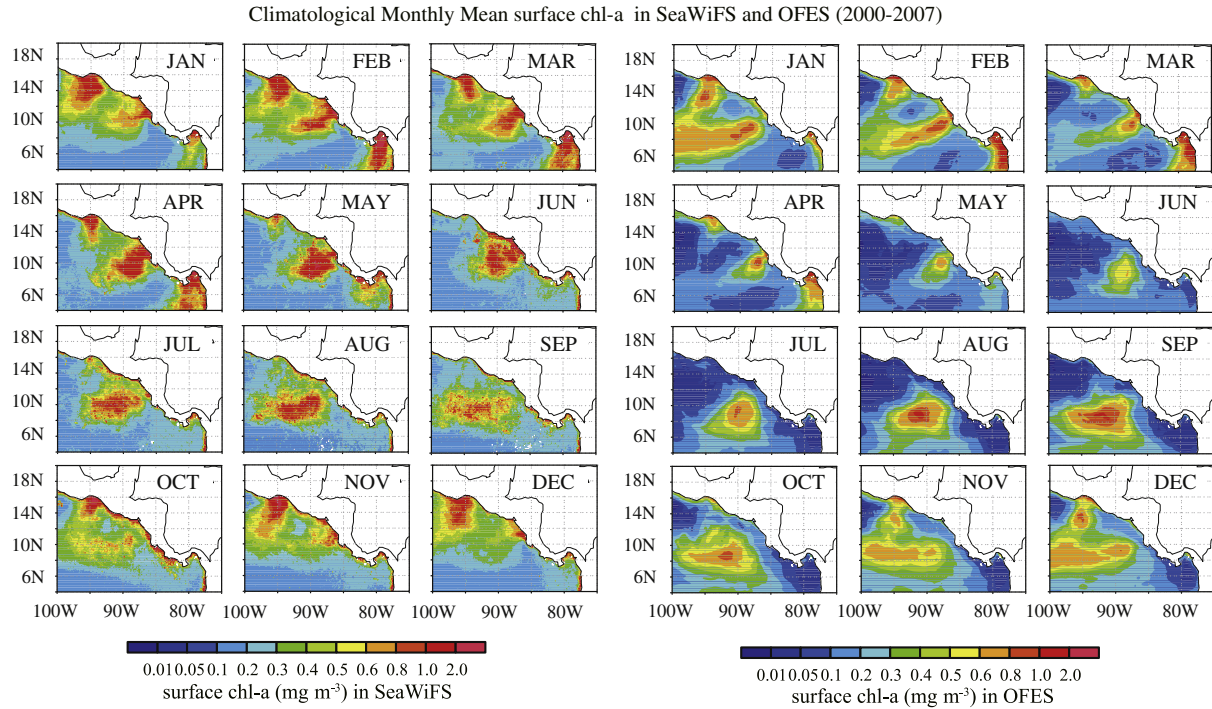


**Fig. 1.** Climatological monthly mean surface chlorophyll concentrations during 2000–2007 from (a) SeaWiFS and (b) OFES.

Observed climatological nitrate concentrations show that the Costa Rica Dome and three Gulfs are enriched by upwelling (Fiedler and Talley, 2006; Peña et al., 1994). The model also represents the seasonal variability of nitrate concentration in the surface layer. During January–April, the model shows that the bloom off the three Gulfs (Fig. 1) overlaps the shoaling of the thermocline depth (<30 m depth) and the high nitrate surface concentrations ( $> 15 \text{ mmol N m}^{-3}$ ) (Figs. 3 and 4), respectively. In the low chlorophyll ( $< 0.2 \text{ mg m}^{-3}$ ) region between the Gulfs of Papagayo and Panama in the model (Fig. 1), the thermocline depth is deep ( $> 60 \text{ m depth}$ ) and the nitrate concentration is low ( $< 5 \text{ mmol N m}^{-3}$ ) (Figs. 3 and 4). In April, the elevation of thermocline off Papagayo begins to look like a dome, but remains connected to the coast (Fig. 3). In May, the shoaling thermocline dome separates from the Gulf of Papagayo. In June, the Costa Rica Dome is distinctly offshore. From June to October, the Costa Rica Dome is shallow and extends westward. The distribution of the offshore blooming varies with the shape of thermocline dome. Inside of the Costa Rica Dome, the high nitrate waters are close to the surface layer and the blooming is maintained (Fig. 4). In November and December, the high nitrate waters at  $6^{\circ}$ – $10^{\circ}\text{N}$  continue to be near the surface layer (Fig. 4) and the surface chlorophyll is still high (Fig. 1). The decrease of observed surface chlorophyll concentration from October to January is not reproduced in the model. The ecosystem model may not represent high nitrate-low chlorophyll condition.

Throughout the year, the variability of thermocline depth is strongly connected with the surface nitrate concentrations. The coastal and open ocean upwelling and the shoaling of the thermocline depth lift up the high nitrate waters to the surface layer and maintain the high chlorophyll concentrations. The monthly mean vertical distribution of simulated chlorophyll and nitrate concentrations along  $10^{\circ}\text{N}$  (Costa Rica Dome and Gulf of Papagayo) is shown in Figs. 5 and 6. A subsurface chlorophyll maximum layer develops between 25 m and 50 m depth in the model. The observed chlorophyll profile (not shown) also shows a maximum at the same depth (shallow near the coast and deep in open ocean) (Chavez et al., 1996; Pennington et al., 2006), although the model overestimates its intensity. The seasonal offshore westward propagation of the chlorophyll maximum in this region is indicative of the propagation of Rossby waves and by the Ekman upwelling from satellite observed data and

model (e.g., Cipollini et al., 2001; McClain et al., 2002; Sasai et al., 2007; Xie et al., 2005). During February–April, the high chlorophyll concentration ( $> 0.8 \text{ mg m}^{-3}$ ) in the model appears between  $90^{\circ}\text{W}$  and  $85^{\circ}\text{W}$  along  $10^{\circ}\text{N}$  (Fig. 5). The strong wind jet in winter over the Gulf of Papagayo causes Ekman upwelling and the upwelling brings cold and high nitrate waters ( $20 \text{ mmol N m}^{-3}$ ) to the surface (Figs. 2, 3, 4, 5 and 6). The maximum chlorophyll waters in the model shoals to 50 m depth and extends to  $90^{\circ}\text{W}$  off the Gulf of Papagayo. Below the wind jet (around  $90^{\circ}\text{W}$ ) (Fig. 2), the high chlorophyll is mixed uniformly in the vertical (Fig. 5). Between  $100^{\circ}\text{W}$  and  $95^{\circ}\text{W}$  along  $10^{\circ}\text{N}$ , the chlorophyll concentration reduces because of the deepening of the thermocline and the nutricline (Figs. 5 and 6). The vertical distributions of chlorophyll and nitrate respond to the wind jet over the Gulf of Papagayo. On the left (right) side of jet, there is upwelling (downwelling) and the thermocline is raised (deepened). Beneath the jet, mixing is enhanced and the mixed layer is deepened. During May–September, the evolution of the chlorophyll signal is strongly influenced by the development of the Costa Rica Dome. The Costa Rica Dome separates from the Gulf of Papagayo in May and shifts near  $90^{\circ}\text{W}$  (Fiedler, 2002a). The center of the dome keeps the dome's waters cold ( $< 20^{\circ}\text{C}$ ) and high in nitrate ( $> 5 \text{ mmol N m}^{-3}$ ) relative to surrounding waters. The thermocline depth is shallow (20 m) and the surface chlorophyll is high by the supply of nitrate-rich waters. In June, the chlorophyll maximum in the subsurface layer along  $10^{\circ}\text{N}$  expands between  $95^{\circ}\text{W}$  and  $87^{\circ}\text{W}$  with the spreading of the Costa Rica Dome. The nitrate-rich water is lifted in the same location by the open ocean upwelling (Fig. 6). During July–September, the high chlorophyll distribution area extends to the west along  $10^{\circ}\text{N}$  and is the same width along  $88^{\circ}\text{W}$  with the spread of the shoaling thermocline (Figs. 5 and 6). The high chlorophyll concentration in the Costa Rica Dome is maintained by the shoaling of nutricline depth ( $5 \text{ mmol N m}^{-3}$ ). During October–December, the maximum chlorophyll layer between 20 m and 40 m depth along  $10^{\circ}\text{N}$  is flat. The nutricline depth is uniformly at 30 m depth. The simulated surface chlorophyll concentration declines as compared with September, but still retains a maximum between  $8^{\circ}$  and  $10^{\circ}\text{N}$  during November–January (Fig. 1).

In the winter months, in contrast, there is no apparent local maximum at  $6^{\circ}$ – $10^{\circ}\text{N}$  in the SeaWiFS chlorophyll (Fig. 1). The reasons for

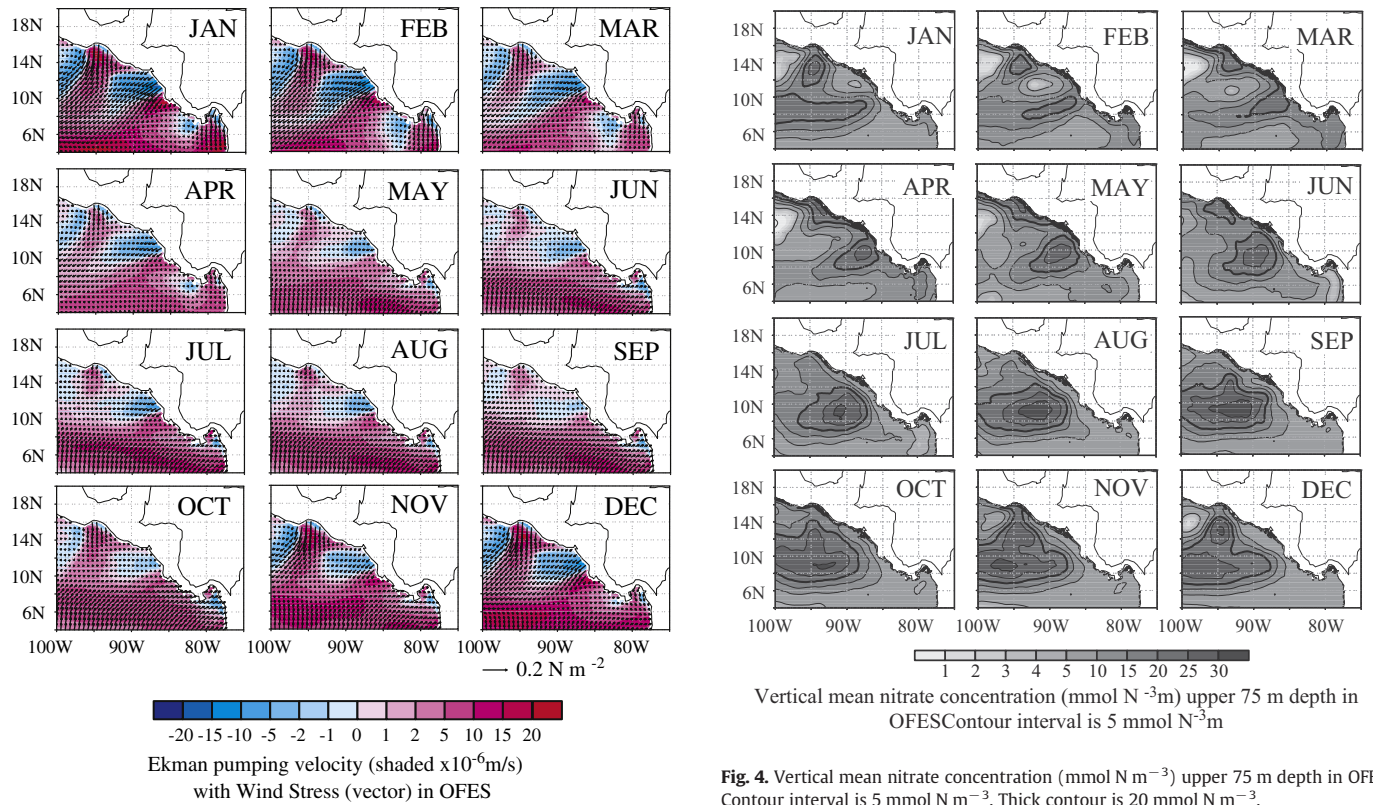


**Fig. 2.** Climatological monthly mean Ekman pumping velocity (color,  $\times 10^{-6} \text{ m s}^{-1}$ ) with wind stress (vector,  $\text{N m}^{-2}$ ) during 2000–2007 from QSCAT.

the differences between model and observations in this region are unclear. As discussed above the model captures the seasonal variation of the ridge in the thermocline depth between  $8^\circ$  and  $10^\circ\text{N}$ . It could

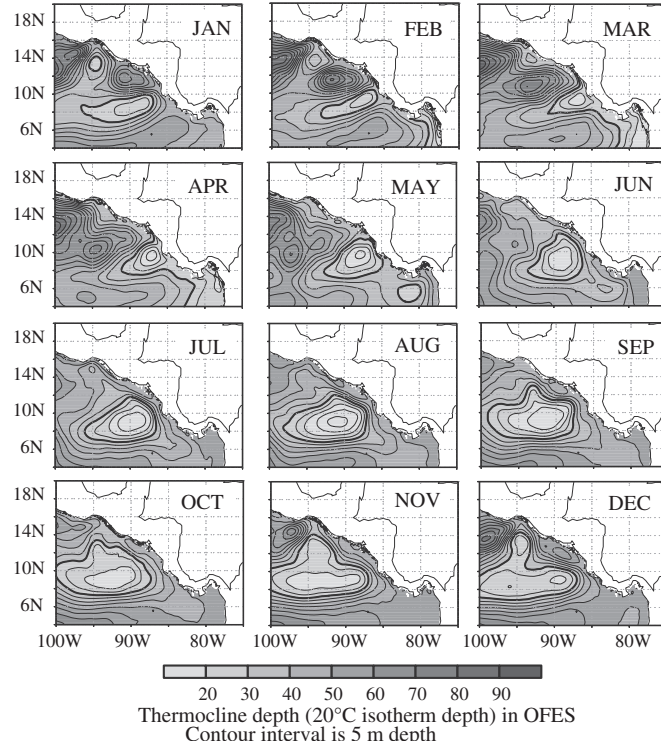


**Fig. 3.** Climatological monthly mean thermocline depth (m) (20°C isotherm depth) in OFES. Contour interval is 5 m depth. Thick contour is 40 m depth.

**Fig. 4.** Vertical mean nitrate concentration ( $\text{mmol N m}^{-3}$ ) upper 75 m depth in OFES. Contour interval is 5  $\text{mmol N m}^{-3}$ .

be that the surface expression of the subsurface chlorophyll in the model is too large, though the vertical distributions of temperature and nitrate in the model are close to the observed climatological data (Fiedler and Talley, 2006). When the supply of nutrient to phytoplankton is increased, the rate of primary production is too high in our ecosystem model compared to observations. This excessive growth is caused by a too high phytoplankton growth rate and/or too low zooplankton grazing pressure. Iron limitation on the phytoplankton growth rate, nitrogen fixation, and a high grazing rate by zooplankton are known to influence the plankton growth rate in the region (e.g., Christian et al., 2002; Karl et al., 1997; Landry et al., 2000; Martin et al., 1994; Pennington et al., 2006) none of which are taken into account in our model.

### 3.2. Interannual variability

There is a strong association of interannual variability of the marine ecosystem in this region with ENSO (e.g., Fiedler, 2002b; Pennington et al., 2006; Wang and Fiedler, 2006). During the warm, El Niño, phase of ENSO, the northeastern tropical Pacific is characterized by weak trade winds, a deep thermocline and warm SST. The cold, La Niña, phase is characterized by strong trade winds, a shallow thermocline and cold SST. ENSO variability can be characterized by the SST monthly anomalies in the Niño 3 region ( $5^\circ\text{S}$ – $5^\circ\text{N}$ ,  $150^\circ\text{W}$ – $90^\circ\text{W}$ ). Fig. 7 shows the comparison of SST monthly anomalies in Niño 3 region between observed data (from the Japan Meteorological Agency) and model. During the analysis period (2000–2007), the variability of SST anomalies in the model shows clearly the same cold (2000–2001, 2007) and warm (2002–2006) SST anomalies as in the observations.

To examine the interannual SST variability in the northeastern tropical Pacific region during 2000–2007, an empirical orthogonal function (EOF) analysis is conducted for the monthly SST anomalies over the 8 yr of the northeastern tropical Pacific (the region is east of  $100^\circ\text{W}$  and north of  $4^\circ\text{N}$ ). The EOF analysis is a statistical method used to decompose a multivariate data set (e.g., time-space data) into an uncorrelated linear combination of separate functions of the original

variables. As a result, a set of spatial modes and associated temporal amplitude functions are obtained. The spatial modes provide information of their spatial structures while the amplitude functions describe their temporal variability. Fig. 8 shows the spatial pattern and temporal variability of first EOF mode of Optimum Interpolation SST (OISST) (Reynolds et al., 2002) and OFES SST anomalies during this period. The first EOF modes of OISST and OFES SST represent 46.1% and 44.8%, respectively, of the total variance. The spatial pattern of the first EOF mode of both OISST and OFES is dominated by a local maximum off the Gulf of Papagayo (Fig. 8a and b). The timeseries of the principal components (PCs) of each (Fig. 8c) follow each other very well, and strongly reflect the large events in the timeseries of Niño 3 SST (Fig. 7). In particular all 4 timeseries (Figs. 7 and 8c) capture the two “warm” events in 2002–03 and 2006–07 and the two “cold” events at the start and end of the timeseries. The next largest “cold” event in the observed Niño 3 SST in 2005–2006 is reflected in the PC1 of OISST, but is small amplitude in the model Niño 3 SST, and is missing in PC1 of OFES.

Fig. 9 shows the spatial pattern and temporal variabilities of the first EOF mode of the observed and simulated monthly chlorophyll anomalies during the same period to examine the interannual variability of surface chlorophyll. The first EOF modes of SeaWiFS and OFES chlorophyll represent 22.8% and 18.5%, respectively, of the total variance. The spatial pattern of the first EOF mode of both SeaWiFS and OFES is dominated by a local extremum off the Gulf of Papagayo (Fig. 9a and b). This spatial pattern is similar to the pattern of the first EOF mode of SST (Fig. 8a and b). The major differences in the EOFs of the observed

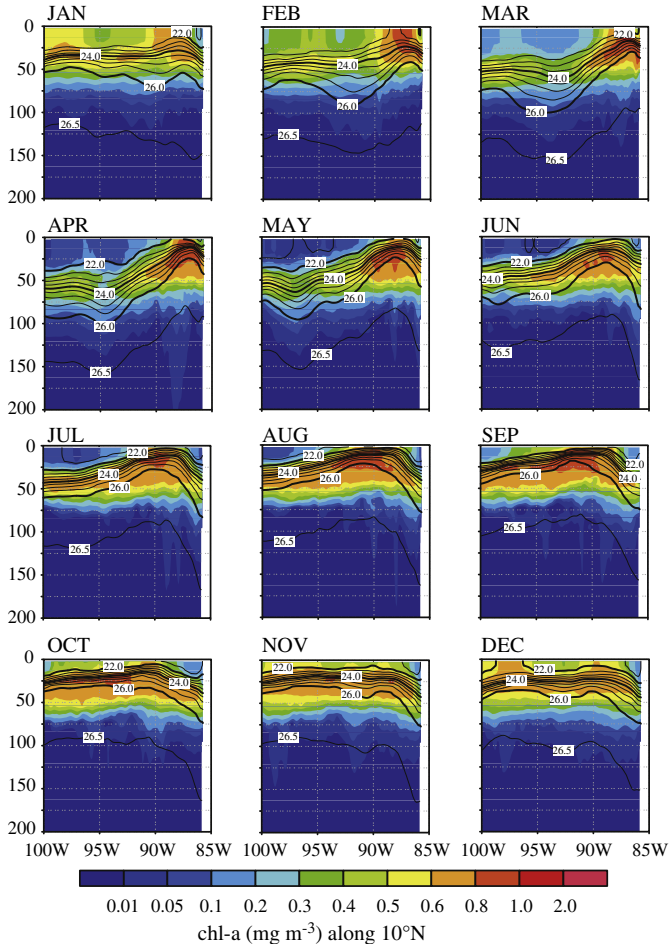


**Fig. 5.** Vertical distribution of climatological monthly mean chlorophyll concentration (color,  $\text{mg m}^{-3}$ ) along  $10^\circ\text{N}$  with potential density (contour). Contour intervals of potential density are 0.5.

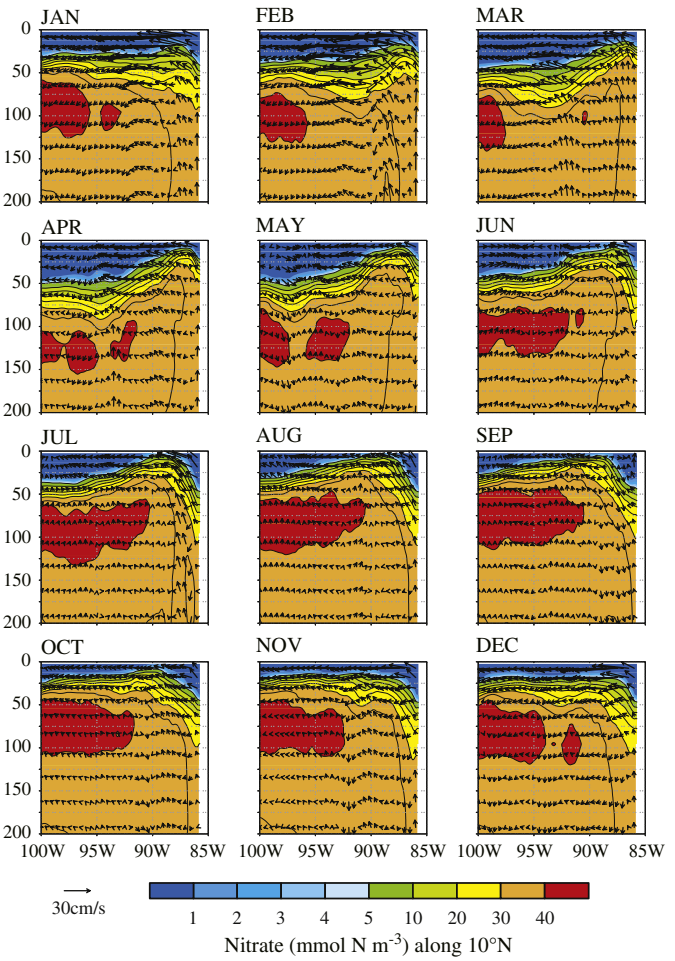


**Fig. 6.** Vertical distribution of climatological monthly mean nitrate concentration (color,  $\text{mmol N m}^{-3}$ ) along (a)  $10^\circ\text{N}$  with vertical velocity ( $\text{cm s}^{-1}$ ). Contour interval is  $5 \text{ mmol N m}^{-3}$ . Vertical velocity is multiplied by  $10^4$ .

and modeled surface chlorophyll are that the extremum off the Gulf of Papagayo extends more to the west in the observed EOF than in OFES and the OFES EOF has a stronger signal to the south of the region. The spatial pattern of SeaWiFS also has a large (negative) value off the Gulf of Tehuantepec.

The timeseries of PC1 of both SeaWiFS and OFES (Fig. 9c) shows the same general variability as the timeseries of PC1 of SST (Fig. 8c). Note, we have chosen the sign convention for the PCs so that a positive PC1 in a given timeseries corresponds to “low” surface chlorophyll and “warm” SST off the Gulf of Papagayo, respectively. The two “low” chlorophyll/“warm” SST events in 2002–03 and 2006–07 (positive PCs; Figs. 9c and 8c) correspond to the two “warm” events in the timeseries of Niño 3 SST (Fig. 7). Likewise the two “high” chlorophyll/“cold” SST events at the start and end of the timeseries (negative PCs; Figs. 9c and 8c) correspond to “cold” Niño 3 SST (Fig. 7). A “low” chlorophyll event in 2004–2005 occurs in both PC1 time series of SeaWiFS and OFES. The same event is seen in the PC1 of the OFES SST but is less distinct in that of the OISST, and non-existent in the Niño 3 SST.

The surface chlorophyll is heavily influenced by the depth of the thermocline and the nutricline. We therefore also present the EOF analysis of the monthly mean  $20^\circ\text{C}$  isotherm depth and  $5 \text{ mmol N m}^{-3}$  nutrient concentration depth of OFES (Fig. 10), which are good indicators of the depth of the thermocline and nutricline, respectively. The first EOF explains 40.9% and 26.9% of the total variance of depths of the thermocline and nutricline, respectively. The spatial pattern of the first EOF mode of the thermocline and nutricline depths shows large variance off the Gulf of Papagayo (Fig. 10a and b). This spatial pattern

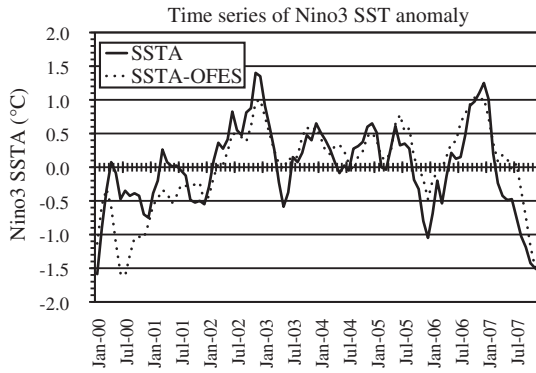


**Fig. 7.** Time series of SST anomalies (2000–2007) in the Niño3 region ( $5^{\circ}\text{S}$ – $5^{\circ}\text{N}$ ,  $150^{\circ}\text{W}$ – $90^{\circ}\text{W}$ ) from observed data (solid line) and OFES (dotted line). The observed SST data is from the Japan Meteorological Agency.

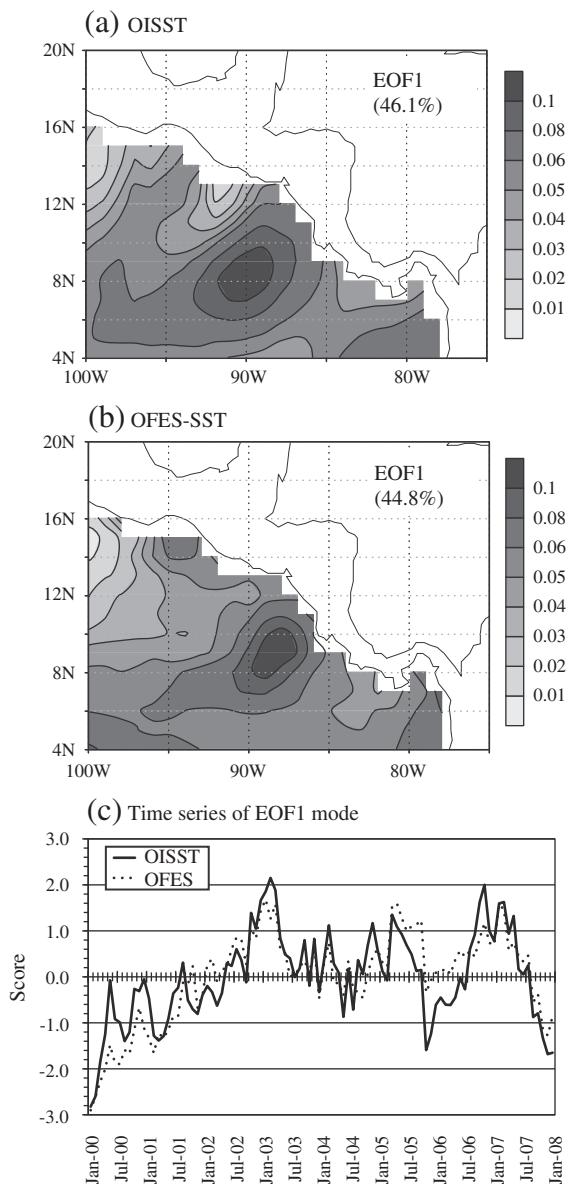


**Fig. 8.** The spatial pattern of first EOF mode of monthly mean (a) OISST (variance is 46.1%) and (b) OFES SST (variance is 44.8%) anomalies during 2000–2007. (c) The temporal variability of first EOF mode of OISST (solid line) and OFES SST (dotted line). The OISST data is obtained from NOAA/National Weather Service web site ([ftp://ftp.emc.ncep.noaa.gov/cmb/sst/oimonth\\_v2/](http://ftp.emc.ncep.noaa.gov/cmb/sst/oimonth_v2/)).

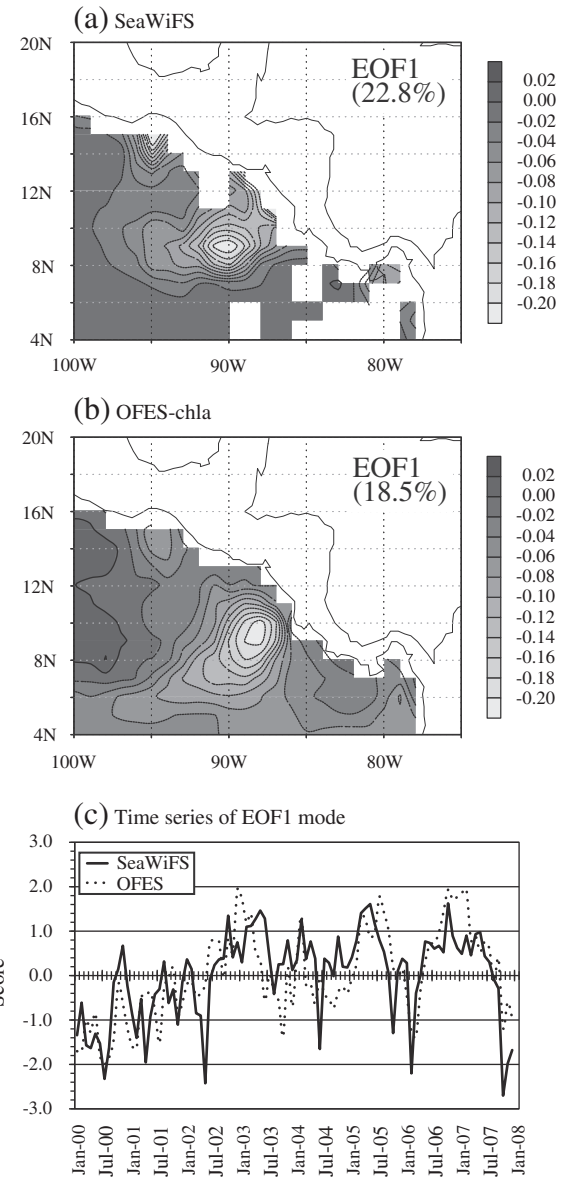


**Fig. 9.** The spatial pattern of first EOF mode of monthly mean (a) SeaWiFS (variance is 22.8%) and (b) OFES chlorophyll concentration (variance is 18.5%) anomalies during 2000–2007. (c) The temporal variability of first EOF mode of SeaWiFS (solid line) and OFES chlorophyll concentration (dotted line).

is the same as the pattern of OFES SST and chlorophyll (Figs. 8b and 9b). The timeseries of PC1 of chlorophyll anomalies (Fig. 9c) shows the same general variability as the timeseries of PC1 of depths of the  $20\ ^{\circ}\text{C}$  isotherm and the  $5\ \text{mmol N m}^{-3}$  nutrient concentration of OFES (Fig. 10c). The positive sign of the PCs correspond to “low” surface chlorophyll, and “deep” thermocline and nutricline, respectively. The large seasonal variation of the spatial pattern of the first EOF mode of chlorophyll corresponds to the development of the Costa Rica Dome. In the OFES, the westward extension of chlorophyll is limited. The spatial pattern of the first EOF mode of OFES SST and thermocline depth show the same pattern as the OFES chlorophyll.

As expected, the spatial pattern and temporal variability of the first EOF mode of the thermocline and nutricline depths are very similar (Fig. 10). In analysis period, there is a strong anticorrelation between the depth of the nutricline and surface chlorophyll; a shallow (deep) nutricline supplying more (less) nutrient to the surface increasing (decreasing) the surface chlorophyll.

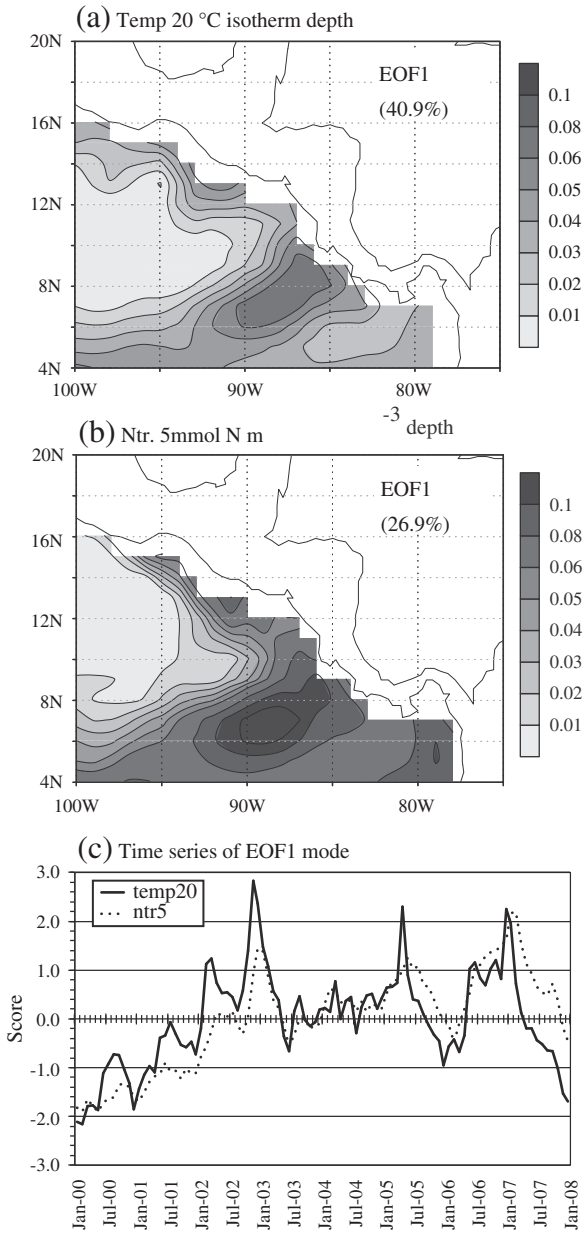


**Fig. 10.** The spatial pattern of first EOF mode of monthly mean (a) OFES thermocline depth ( $20^{\circ}\text{C}$  isotherm depth) anomalies (variance is 40.9%) and (b) OFES nutricline depth ( $5 \text{ mmol N m}^{-3}$  depth) anomalies (variance is 26.9%) during 2000–2007. (c) The temporal variability of first EOF mode of thermocline depth (solid line) and nutricline depth (dotted line).

Lastly, as shown in Fig. 6 there is a strong sub-surface maximum in chlorophyll in the region of the Costa Rica Dome (Fig. 5), a region that is very prominent in the spatial structure of the interannual variability (Figs. 8, 9, and 10). In Fig. 11a we compare the temporal variations of the surface and the depth averaged ( $0\text{--}50 \text{ m}$ ) chlorophyll concentrations averaged over the Costa Rica Dome region. Variations in the surface concentration reflect well the variations in the total chlorophyll, both of which are strongly related to variations in the depth of the thermocline (Fig. 11b).

#### 4. Conclusion

The complex physical environment of both ocean and atmosphere strongly impacts on seasonal and interannual variations of the marine ecosystem in the northeastern tropical Pacific. We have investigated

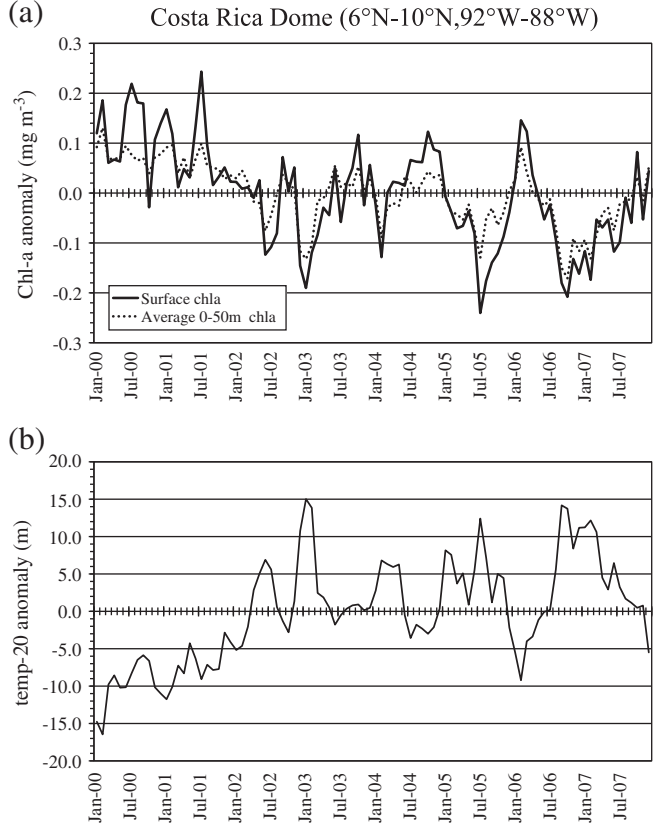


**Fig. 11.** Timeseries of (a) surface chlorophyll (solid line) and average  $0\text{--}50 \text{ m}$  chlorophyll ( $\text{mg m}^{-3}$ ) concentration anomalies of OFES, and (b) thermocline ( $\text{m}$ ,  $20^{\circ}\text{C}$  isotherm depth) depth anomaly of OFES in the area-averaged Costa Rica Dome ( $6^{\circ}\text{N}$ – $10^{\circ}\text{N}$ ,  $92^{\circ}\text{W}$ – $88^{\circ}\text{W}$ ) during 2000–2007.

these variations using observations and an eddy-resolving physical–biological model. During 2000–2007, the period of the present study, the model clearly captures the observed seasonal cycle of surface chlorophyll concentration which is induced by seasonal variations in vertical mixing and Ekman pumping produced by the surface wind, the ocean circulation, and changes to the depth of the thermocline. The spatial pattern of seasonal variations of surface chlorophyll reflects the pattern of variation in the thermocline depth and subsurface nitrate concentration. High chlorophyll levels off the Gulf of Tehuantepec in October–March and Gulf of Papagayo in January–April are caused by the uplifted thermocline and elevated nutrient levels induced by the winter wind jets. The surface chlorophyll offshore is influenced by evolution of the Costa Rica Dome. During June–September, high chlorophyll develops offshore along the shoaling thermocline ridge, with a local maximum corresponding to the Costa Rica Dome. In the center of the thermocline dome, the nitrate rich-waters are uplifted and a high chlorophyll condition is maintained.

Much of the spatial pattern of the seasonal cycle in surface chlorophyll, and its relationship with SST and the depth of the thermocline, is present in the large interannual variations in the region. A substantial amount of this interannual variability is strongly linked to ENSO in both observations and the model results. Cold ENSO events are associated with a cooler local SST pattern and increased surface chlorophyll concentration. The reverse is true for warm ENSO events. There is a strong anticorrelation between the depth of the thermocline (and nutricline) and the surface chlorophyll. Interannual variability in the fall and winter is associated with variations in the wind jets. Variability in the spring and summer is associated with variation in the strength of the Costa Rica Dome.

Over a similar period to the present study Behrenfeld et al. (2006) find a strong anticorrelation in satellite derived global fields of SST

and surface chlorophyll with a distinct downward trend in the globally averaged chlorophyll anomaly after 1999. The reason proposed for the anticorrelation is the increase in stratification of the surface layers of the ocean as the planet warms. It is noteworthy we find the same anticorrelation between SST and surface chlorophyll although the link between the two is through interior ocean physics resulting in variations in the depth of the thermocline. Our study points to the need for further regional studies to investigate the link between chlorophyll and ocean physics on interannual and longer timescales.

## Acknowledgment

We thank Drs. Yukio Masumoto, Takashi Kagimoto, and Shintaro Kawahara for their collaborations in extending the OFES model for biological research. The QSCAT product of J-OFURO was obtained from Prof. Kunio Kutsuwada. Using ocean color satellite data was obtained from Dr. Kosei Sasaoka. OFES simulations were conducted on the Earth Simulator under the support of JAMSTEC. This work was partly supported by CREST, JST.

## References

- Amador, J.A., Alfaro, E.J., Lizano, O.G., Magaña, V.O., 2006. Atmospheric forcing of the eastern tropical Pacific: a review. *Prog. Oceanogr.* 69, 101–142.
- Barber, R.T., Ryther, J.H., 1969. Organic chelators: factors affecting primary production in the Cromwell Current upwelling. *J. Exp. Mar. Biol. Ecol.* 3, 191–199.
- Behrenfeld, M.J., O'Malley, R.T., Siegel, D.A., McClain, C.R., Sarmiento, J.L., Feldman, G.C., Milligan, A.J., Falkowski, P.G., Letelier, R.M., Boss, E.S., 2006. Climate-driven trends in contemporary ocean productivity. *Nature* 444, 752–755.
- Bruland, K.W., Rue, E.L., Smith, G.J., DiFulio, G.R., 2005. Iron, macronutrients and diatom blooms in the Peru upwelling regime: brown and blue waters of Peru. *Mar. Chem.* 93, 81–103.
- Chavez, F.P., 1989. Size distribution of phytoplankton in the central and eastern tropical Pacific. *Global Biogeochem. Cycles* 3, 27–35.
- Chavez, F.P., Buck, K.R., S.K. Service, Newton, J., Barber, R.T., 1996. Phytoplankton variability in the central and eastern tropical Pacific. *Deep-Sea Res. II* 43, 835–870.
- Chavez, F.P., Strutton, P.G., Friederich, G.E., Feely, R.A., Feldman, G.C., Foley, D.G., McPhaden, M.J., 1999. Biological and chemical response of the equatorial Pacific Ocean to the 1997–98 El Niño. *Science* 286, 2126–2131.
- Chelton, D.B., Freilich, M.H., Esbensen, S.K., 2000. Satellite observations of the wind jets off the Pacific coast of Central America. Part I: Case studies and statistical characteristics. *Mon. Wea. Rev.* 128, 1993–2018.
- Chelton, D.B., Schlax, M.G., Freilich, M.H., Milliff, R.F., 2004. Satellite measurements reveal persistent small-scale features in ocean winds. *Science* 303, 978–983.
- Christian, J.R., Verschell, M.A., Murtugudde, R., Busalacchi, A.J., McClain, C.R., 2002. Biogeochemical modeling of the tropical Pacific Ocean II: Iron biogeochemistry. *Deep-Sea Res. II* 49, 545–565.
- Cipollini, P., Cromwell, D., Challenor, P.G., Raffaglio, S., 2001. Rossby waves detected in global ocean color data. *Geophys. Res. Lett.* 28 (2), 323–326.
- Cloern, J.E., Grenz, C., Vidérigar-Lucas, L., 1995. An empirical model of the phytoplankton chlorophyll: carbon ratio—the conversion factor between productivity and growth rate. *Limnol. Oceanogr.* 40, 1313–1321.
- Dugdale, R.C., Wilkerson, F.P., Minas, H.J., 1995. The role of silicate pump in driving new production. *Deep-Sea Res. I* 42, 697–719.
- Fasham, M.J.R., Ducklow, H.W., McKelvie, S.M., 1990. A nitrogen-based model of phytoplankton dynamics in the oceanic mixed layer. *J. Mar. Res.* 48, 591–639.
- Fiedler, P.C., 2002a. The annual cycle and biological effects of the Costa Rica Dome. *Deep-Sea Res. I* 49, 321–338.
- Fiedler, P.C., 2002b. Environmental change in the eastern tropical Pacific Ocean: review of ENSO and decadal variability. *Mar. Ecol. Prog. Ser.* 244, 265–283.
- Fiedler, P.C., Talley, L.D., 2006. Hydrography of the eastern tropical Pacific: a review. *Prog. Oceanogr.* 69, 143–180.
- Fiedler, P.C., Philbrick, V., Chavez, F.P., 1991. Oceanic upwelling and productivity in the eastern tropical Pacific. *Limnol. Oceanogr.* 36, 1834–1850.
- Gonzalez-Silveira, A., Santamaría-de-Angel, E., Millán-Núñez, R., Manzo-Monroy, H., 2004. Satellite observations of mesoscale eddies in the Gulfs of Tehuantepec and Papagayo (Eastern Tropical Pacific). *Deep-Sea Res. II* 51, 587–600.
- Kalnay, E., Kanamitsu, M., Kistler, R., et al., 1996. The NCEP/NCAR 40-year reanalysis project. *Bull. Am. Meteorol. Soc.* 77, 437–471.
- Karl, D., Letelier, R., Tupas, L., Dore, J., Christian, J., Hebel, D., 1997. The role of nitrogen fixation in the biogeochemical cycles in the subtropical North Pacific Ocean. *Nature* 388, 533–538.
- Kessler, W.S., 2002. Mean three-dimensional circulation in the northeast tropical Pacific. *J. Phys. Oceanogr.* 32, 2457–2471.
- Kessler, W.S., 2006. The circulation of the eastern tropical Pacific: a review. *Prog. Oceanogr.* 69, 181–217.
- Landry, M.R., Kirchman, D.L., 2002. Microbial community structure and variability in the tropical Pacific. *Deep-Sea Res. II* 49, 2669–2693.
- Landry, M.R., Constantinou, J., Lataza, M., Brown, S.L., Bidigare, R.R., Ondrussek, M.E., 2000. Biological response to iron fertilization in the eastern equatorial Pacific (IronEx II). III. Dynamics of phytoplankton growth and microzooplankton grazing. *Mar. Ecol. Prog. Ser.* 201, 57–72.
- Martin, J.H., Coale, K.H., Johnson, K.S., Fitzwater, S.E., Gordon, R.M., Tanner, S.J., Hunter, C.N., Elrod, V.A., Nowicki, J.L., Barber, R.T., Lindley, S., Watson, A.J., Van Skoy, K., Law, C.S., Liddicoat, M.J., Ling, R., Santon, T., Stockel, J., Collins, C., Anderson, A., Bidigare, R., Ondrussek, M., Lataza, M., Millero, F., Lee, K., Yao, W., Zhang, J., Frederich, G., Sakamoto, C., Chavez, F., Buck, K., Kolber, Z., Greene, R., Falkowski, P., Chisolm, S.W., Hoge, F., Swift, R., Yungel, J., Turner, S., Nightingale, P.D., Hatton, A., Liss, P., Tondale, N.W., 1994. Testing the iron hypothesis in ecosystems of the equatorial Pacific Ocean. *Nature* 371, 123–129.
- Masumoto, Y., Sasaki, H., Kagimoto, T., Komori, N., Ishida, A., Sasai, Y., Miyama, T., Motoi, T., Mitsudera, H., Takahashi, K., Sakuma, H., 2004. A fifty-year-eddy-resolving simulation of the world ocean: preliminary outcomes of OFES (OGCM for the Earth Simulator). *J. Earth Simulator* 1, 35–56.
- McClain, C.R., Christian, J.R., Signorini, S.R., Lewis, M.R., Asanuma, I., Turk, D., Dupouy-Douchement, C., 2002. Satellite ocean-color observations of the tropical Pacific Ocean. *Deep-Sea Res. II* 49, 2533–2560.
- Müller-Karger, F.E., Fuentes-Yaco, C., 2000. Characteristics of wind-generated rings in the eastern tropical Pacific Ocean. *J. Geophys. Res.* 105, 1271–1284.
- Oschlies, A., 2001. Model-derived estimates of new production: new results point towards lower values. *Deep-Sea Res. II* 48, 2173–2197.
- Pacanowski, R.C., Griffies, S.M., 2000. MOM 3.0 Manual. Geophysical Fluid Dynamics Laboratory/National Oceanic and Atmospheric Administration. 680 pp.
- Peña, M.A., Lewis, M.R., Cullen, J.J., 1994. New production in the warm waters of the tropical Pacific Ocean. *J. Geophys. Res.* 99, 14255–14268.
- Pennington, J.T., Mahoney, K.L., Kuwahara, V.S., Kolber, D.D., Calienes, R., Chavez, F.P., 2006. Primary production in the eastern tropical Pacific: a review. *Prog. Oceanogr.* 69, 285–317.
- Reynolds, R.W., Raynet, N.A., Smith, T.M., Stokes, D.C., Wang, W., 2002. An improved in situ and satellite SST analysis for climate. *J. Climate* 15, 1609–1625.
- Ryan, J.P., Polito, P.S., Strutton, P.G., Chavez, F.P., 2002. Unusual large-scale phytoplankton blooms in the equatorial Pacific. *Prog. Oceanogr.* 55, 263–285.
- Samuelsen, A., O'Brien, J.J., 2008. Wind-induced cross shelf flux of water masses and organic matter at the Gulf of Tehuantepec. *Deep-Sea Res. I* 55, 221–246.
- Sasai, Y., Ishida, A., Sasaki, H., Kawahara, S., Uehara, H., Yamanaka, Y., 2006. A global eddy-resolving coupled physical and biological model: physical influences on a marine ecosystem in the North Pacific. *Simulation* 82, 467–474.
- Sasai, Y., Sasaki, H., Sasaoka, K., Ishida, A., Yamanaka, Y., 2007. Marine ecosystem simulation in the eastern tropical Pacific with a global eddy resolving coupled physical-biological model. *Geophys. Res. Lett.* 34, L23601. doi:10.1029/2007GL031507.
- Sasai, Y., Richards, K.J., Ishida, A., Sasaki, H., 2010. Effects of cyclonic mesoscale eddies on the marine ecosystem in the Kuroshio Extension region using an eddy-resolving coupled physical-biological model. *Ocean Dyn.* 60 (3), 693–704. doi:10.1007/s10236-010-0264-8.
- Strutton, P.G., Chavez, F.P., 2000. Primary productivity in the equatorial Pacific during the 1997–1998 El Niño. *J. Geophys. Res.* 105, 26089–26101.
- Wang, C., Fiedler, P.C., 2006. ENSO variability and the eastern tropical Pacific: a review. *Prog. Oceanogr.* 69, 239–266.
- Willett, C.S., Leben, R.R., Lavin, M.F., 2006. Eddies and tropical instability waves in the eastern tropical Pacific: a review. *Prog. Oceanogr.* 69, 218–238.
- Xie, S.-P., Xu, H., Kessler, W.S., Nonaka, M., 2005. Air-sea interaction over the eastern Pacific warm pool: gap winds, thermocline dome, and atmospheric convection. *J. Climate* 18, 5–20.